Controlling covalent chemistry on graphene oxide

Shi Guo, Slaven Garaj, Alberto Bianco, Cécilia Ménard-Moyon

Controlling covalent chemistry on graphene oxide

Shi Guo[1], Slaven Garaj[2], Alberto Bianco[1] and Cécilia Ménard-Moyon[1,†]

[1]CNRS, Immunology, Immunopathology and Therapeutic Chemistry, UPR3572, University of Strasbourg, ISIS, Strasbourg, France.

[2]Department of Physics, Department of Biomedical Engineering and Department of Materials Science and Engineering, National University of Singapore, Singapore, Singapore.

[†]email: c.menard@ibmc-cnrs.unistra.fr

Toc Blurb

Graphene oxide (GO) has attracted intensive research interest owing to remarkable physicochemical properties. Nevertheless, its high chemical reactivity and low stability may lead to uncontrolled GO derivatives. The chemistry of GO can be controlled by selective derivatization of the oxygenated groups and C=C bonds, and by appropriate characterization.

Abstract

Graphene has attracted intensive research interest in many fields owing to its remarkable physicochemical properties. Nevertheless, its low dispersibility in most organic solvents and in water, and its tendency to aggregate, prevent full exploitation of its properties. Graphene oxide (GO) is an alternative material that exhibits high dispersibility in polar solvents. GO contains abundant oxygen-containing groups, mainly epoxide and hydroxy groups, which can be further chemically derivatized. However, because of GO's high reactivity, several reactions may occur simultaneously, often leading to uncontrolled GO derivatives. Moreover, because GO can be easily reduced, functionalization should be performed under mild conditions. In this Review, we discuss the chemical reactivity of GO and explore issues that hamper precise control of its functionalization, such as the lack of a well-defined chemical structure, its instability and the presence of impurities. We focus on strategies for the selective derivatization of the oxygenated groups and C=C bonds, along with the challenges for unambiguous characterization of the resulting structures. We briefly review applications of GO materials, relating their chemistry and

nanostructure to desired physical properties and function, and chart future directions for improving the control of GO chemistry.

Key points

- Graphene oxide (GO) contains abundant oxygenated groups, mainly epoxide and hydroxy groups on the basal plane, with a small number of carboxyl moieties at the edges.
- The functionalization of GO must be performed under mild conditions to avoid dehydration and reduction, which can occur upon heating or in the presence of a strong base.
- Chemoselective reactions are crucial in controlling the derivatization of GO, owing to the high reactivity of the different oxygenated groups, which gives rise to potential side reactions and, thus, uncontrolled GO chemical structures.
- Unambiguous characterization of GO is challenging. The conjugation of elements or functional groups that can be unambiguously identified onto the surface of GO can facilitate characterization.
- The intrinsic properties of GO, including a high proton conductivity and water dispersibility, must be preserved after functionalization for some applications, such as proton-exchange membranes for fuel cells or membranes for water filtration.

Introduction

For more than 15 years, graphene has attracted interest in diverse fields owing to its unique optical, electrical, thermal and mechanical properties[1]. However, the low dispersibility of graphene in most organic solvents and in water, and its propensity to aggregate, limits its processability. Moreover, the sp^2 basal plane of graphene is relatively inert, inhibiting its covalent functionalization and thus restricting its range of applications. By contrast, the oxidized form of graphene — graphene oxide (GO) — has high dispersibility in many solvents[2], and the abundant oxygenated moieties provide handles for a wide range of chemical derivatizations[3]. These properties facilitate processing and enable the low-cost and scalable production of GO materials. GO consists of flexible 2D graphitic flakes (‘macromolecules’) with atomic thickness (~1 nm) and lateral dimensions on the nanometre-to-micrometre scale. The surface of GO is decorated with oxygenated groups: numerous epoxide and hydroxy (–OH) moieties are mainly located on the basal plane, while a few carboxyl (–COOH) groups are present at the edges.

It is essential to understand that GO is not a single chemical compound, but rather a class of heterogeneous materials. The physical and chemical properties of GO, and corresponding applications, are defined by its composition and structure at different scales (Fig. 1a). The properties depend on the details of the chemistry (for example, the level of oxidation, the ratio and localization of oxygenated groups, and the number of residual non-oxygen groups), the density of defects and nanopores, and the distribution and clustering of functional groups[4]. The properties of GO can be further modified by changing the microscopic structure, namely the flake size distribution and relative arrangement of the flakes (such as liquid-suspended flakes, hydrogels or laminates). This hierarchical composition determines the optical and electrical properties, as well as the liquid, ion and gas transport properties of GO-based materials[5-7].

Chemical modifications of GO provide opportunities to controllably change the properties of the associated materials, improving their performance in many applications, including in environmental[8] and energy-related fields[9], polymer composites[10], sensing[11], filtration[12], catalysis[13] and nanomedicine[14]. However, because GO is unstable upon heating and in the presence of strong bases, functionalization must be performed under neutral and mild conditions to avoid the dehydration and reduction of GO. Owing to the relatively high reactivity of the oxygenated groups in GO, several reactions can proceed concomitantly during the functionalization, possibly leading to side reactions and resultant materials with an ill-defined composition. Therefore, synthetic strategies are needed for controlled functionalization of GO and techniques are required for accurate characterization of the functionalized materials.

In this Review, we give an overview of the chemical reactivity of GO and discuss the factors that impede precise control of the functionalization of GO; these include the absence of a well-defined chemical structure of the GO macromolecule, its thermal instability, its incompatibility with strong bases, and the potential presence of impurities. We detail the approaches for the selective covalent derivatization of the different oxygenated groups and the C=C bonds, with a focus on facilitating understanding of the reactivity rather than mechanistic details. Our discussion is limited to covalent chemistry, as it gives GO conjugates that are more stable than those derived from non-covalent interactions[15]. Failure to grasp the heterogeneity of GO materials often leads to erroneous conclusions and miscommunication in the literature. In this regard, we consider the challenges in characterizing GO and highlight the procedures and techniques that can be used to unambiguously characterize GO materials. Finally, we explore the structure–function relationships

of functionalized GO in the context of example applications in environmental and energy-related fields.

Challenges of chemistry on graphene oxide

GO can be prepared by different methods. The most widely used synthetic protocol was proposed in 1958 by Hummers and Offeman and uses strong oxidizing agents and concentrated acids[4,16,17]; these harsh conditions allow for the oxidative exfoliation of graphite.

Structure and composition

The structure of GO is heterogeneous and is mainly composed of aromatic graphitic islands, constituted of unoxidized condensed benzene rings, and oxidized sp^3 carbon atom regions with aliphatic six-membered rings[18] (Fig 1b,c). The chemical composition of both domains and their relative size depend on the degree of oxidation. Thus, there exists no exact structure of GO, and its chemical structure is still under debate[19,20].

The most widely accepted structural model of GO, prepared by oxidative chemical exfoliation of graphite using potassium permanganate, was suggested by Lerf, Klinowski and colleagues in 1998 (ref.[21]). In this 'Lerf–Klinowski' model, the graphene basal plane is functionalized with epoxide and hydroxy groups, with a smaller number of carbonyl (C=O) and carboxyl groups located at the edges as a consequence of C–C bond breaking owing to overoxidation[22,23] (Fig. 1d). Subsequently, this model has been updated, with other functionalities and features, such as lactols, carbon vacancies, sulfate esters, carbon radicals and C–H bonds, having been identified[24-26]. The basal plane of GO contains topological defects, including holes ($<5\ nm^2$) caused by vacancy defects, the density of which depends on the oxidation level[27,28] (Fig. 1c). Sulfate groups (C–O–SO_3^-) arise from the nucleophilic opening of the epoxides by sulfuric acid or hydrogen sulfate, and their hydrolysis is slow[29,30]. The presence of sulfate groups in GO can be explained by incomplete hydrolysis during the aqueous work-up. Therefore, the sulfate content depends on the thoroughness of the aqueous washing, and it may vary between batches. For example, the sulfur content is <1 atomic.% in thoroughly washed GO, whereas it is 1.5–2.5 at.% in moderately washed samples[30,31]. Freshly prepared GO can also contain numerous π-conjugated carbon radicals that are temporarily stabilized by the conjugation[32,33]. Endoperoxides can be present[34] and may be toxic to

cells and, thus, problematic for biomedical applications. The three main domains of GO — intact sp^2-conjugated islands (for non-overoxidized GO, generally ~50% of carbon atoms are sp^2 hybridized), oxidized aliphatic carbon regions and holes — are randomly distributed[35].

In addition to the commonly used Hummers' method, for which many improvements have been reported (named modified Hummers' methods)[36], other protocols have also been developed to synthesize GO[37-39]. However, these methodologies use different oxidation conditions, and graphite precursors of varying types and sizes[40] produce GO with a different number and ratio of oxygenated groups. GO has a non-stoichiometric molecular formula: $C_xH_yO_z$, with $y = 0.8$ and the C/O ratio (x/z) varying between 1.5 and 2.5 (for $z = 1$)[4]. Hence, the main issue relating to the chemistry of GO is the determination of the type and number of oxygenated groups and the number of defects.

The surface of GO flakes that contain mainly C=C bonds, aromatic entities and epoxides are nearly flat. By contrast, carbon atoms that bear hydroxy groups adopt a slightly distorted tetrahedral configuration, which causes wrinkling of the sheets[41] and hinders electron delocalization, thus resulting in a lower electrical conductivity compared with graphene. Furthermore, the distortion of the graphene lattice can increase its chemical reactivity[43]. The oxygenated groups also affect the electronic structure of GO, as epoxides remove two π electrons from nearby sublattice sites and carbonyl functions add an additional electron to the π-conjugated system, decreasing the conductivity[42]. The sp^2-carbon patches in GO can behave as confined electronic environments, resulting in band-gap opening[44], which can overcome the limitations associated with the zero band gap of graphene.

Impurities and instability

Trace amounts of metallic impurities can be found in GO, arising from the graphite or the chemical reagents used for the oxidation[4]. In the case of overoxidation, small, highly oxidized polyaromatic fragments can be cleaved from the GO sheets and adsorbed onto the surface. These fragments can be removed by base washing[45-47]. Nevertheless, the origin of these oxidized debris is still controversial[48].

The stability of GO suspensions is influenced by the equilibrium between the attractive van der Waals force and repulsive electrostatic interactions between the sheets[49]. Therefore, protonation of the oxygenated groups at acidic pH decreases the electrostatic repulsion between

GO layers and induces aggregation in aqueous solutions[50]. Conversely, GO is deprotonated at basic pH and the suspensions are stable, whereas the sheets tend to fold owing to the electrostatic repulsion between the negatively charged GO flakes. The structure of GO is dynamic, in particular when stored in water[51]. Indeed, water is a nucleophile that can react with GO and lead to C–C bond cleavage, increased conjugation and the generation of protons, which could explain the acidity of aqueous GO suspensions[29,52]. This process is rather slow, but should be taken into consideration for the long-term storage (>1 year) of GO in water. In powder form, GO is more stable if stored under an inert atmosphere[53]. Nevertheless, upon drying, the GO sheets tend to aggregate, thus drastically decreasing the specific surface area.

The structure of GO can change in alkaline aqueous solutions, as the hydroxide ions can open the epoxide rings, even at room temperature[54]. This reaction is reversible at room temperature, as the epoxides can be recovered after acidic treatment. Nonetheless, even at 40 °C, GO is unstable after treatment with sodium hydroxide, which leads to rupture of the carbon framework[55]. Above 70 °C, the epoxide ring-opening reaction is irreversible, and treatment with hydroxide ions leads to the reduction of GO or the introduction of defects, which might result in disintegration of the flakes, depending on the conditions[56,57]. Both theoretical simulations[52,58] and experiments[54] have revealed that epoxide ring opening following alkaline treatment of GO leads to the formation of diols. The diol-attached C–C bonds can be decomposed, generating carboxyl groups and CO_2, which results in the reduction of GO, or more precisely its deoxygenation, and in an increase in the graphitic carbon content.

GO is also thermally unstable, and heating the material to above 80 °C can modify its composition, increasing the C/O ratio and thus inducing partial reduction[59]. The formation of CO_2 has been observed at temperatures as low as 50 °C and generates hole defects[60].

Overall, the complex chemical structure of GO is associated with instability and potential impurities, making functionalization difficult to control and to elucidate.

Chemoselective functionalization

Functionalization of GO enables the fine tuning of its physicochemical properties. The chemistry of GO is mainly inspired by classic organic transformations of epoxide, hydroxy and carboxyl groups, as well as C=C bonds. Here, we focus on the main reactions that enable the chemoselective

derivatization of these functional groups while preserving the intrinsic properties of GO. We have selected reactions that are chemoselective, do not induce GO reduction, and for which a chemically correct structure was reported. Because of the thermal instability of GO and its reduction by strong bases, controlled and mild reaction conditions must be used to achieve chemoselectivity. Thus, we focus on reactions performed under mild conditions and do not discuss those performed under harsh conditions. We consider the selective derivatization of epoxide, hydroxy and other oxygenated groups, and C=C bonds, in turn, before discussing strategies for the multifunctionalization of GO. Table 1 summarizes the main advantages and limitations of the reactions reported below for the derivatization of GO (see Table S1 of the Supplementary Information for further details). In addition to these reactions, various strategies have also been reported for the halogenation of GO (section 1.5 of the Supplementary Information).

Epoxide opening

As epoxide and hydroxy moieties are abundant on the surface of GO, most functionalization strategies target these functional groups. Nucleophilic attack at the carbon atom of an epoxide, occurring from the backside of the GO layer, releases the ring strain and forms a new bond between the nucleophile and the carbon atom of GO, in addition to the formation of a new hydroxy group on the basal plane of GO (Fig. 2a). Amines, thiols and the azide anion (N_3^-) are examples of nucleophiles that are highly reactive towards the epoxides[61-63]. Indeed, the reaction between amines and epoxides is widely used beyond GO, such as in polymer science to cure epoxy resins. The introduction of azides allows for further functionalization through copper(I) catalysed azide–alkyne cycloaddition (the so-called click reaction) with molecules that contain C≡C bonds, provides the means to introduce a wider range of functional groups[64]. Particular attention must be paid to avoiding the use of highly basic carbanion nucleophiles to open the epoxides, as these can substantially reduce GO[65]. Nucleophilic epoxide ring opening is the most practical method to functionalize GO, as it is simple to perform and occurs under mild and environmentally friendly conditions (in water, at room temperature and without catalysts).

Hydroxy group derivatization

Although hydroxy groups are not particularly reactive nucleophiles or electrophiles, they can still participate in many chemical reactions. The most common method to derivatize GO through the

hydroxy functions is silanization, which involves the reaction with organosilanes to form covalent Si–O bonds[66] (Fig. 3a). This reaction is widely used to functionalize mineral components, such as glass and metal oxide surfaces, with many applications in coatings and materials science. The detailed mechanism of silanization is controversial: it is not fully understood and depends on the reaction conditions. This reaction occurs spontaneously without a catalyst but has some limitations. First, the use of silanes that contain amines or thiols should be avoided to prevent side reactions with the epoxides. Moreover, trialkoxysilanes can polymerize in the presence of water and at high concentration, forming oligomers and polymers that can attach to the GO surface. Another issue is the potential involvement of the GO carboxyl groups in the silanization, highlighting the limited chemoselectivity of this method. Nevertheless, the functionalization of GO with organosilanes is an important strategy to produce graphene–silica composites, which can be used as reinforcement in polymer nanocomposites, for example. Another extensively used reaction to derivatize GO involves chlorosulfonic acid (HSO_3Cl) to transform the hydroxy groups into organosulfates (–C–O–SO_2–OH), thus allowing the preparation of sulfated GO[67].

Other reactions can also be employed for the derivatization of the hydroxy functions of GO. For instance, boronic acids are highly reactive towards 1,2-diols and 1,3-diols. This reaction occurs under slightly alkaline conditions and forms cyclic boronic esters[68] (Fig. 3b). Alternatively, the reaction can be performed by heating (80–120 °C) to avoid using an alkaline solution, but might lead to partial reduction of GO[69]. The functionalization of GO with boronic acid derivatives can be used to form frameworks for various applications, such as fuel cells, filtration, gas storage and supercapacitors[68,69,70,71]. However, boronic esters can be cleaved at acidic pH, which could be a limitation for some applications.

The hydroxy groups can also react with molecules bearing a carboxyl group to form ester bonds[72] (Fig. 3c). However, coupling agents, including *N*-(3-dimethylaminopropyl)-*N′*-ethylcarbodiimide and 1-hydroxybenzotriazole or *N*-hydroxysuccinimide, are required to activate the carboxyl groups. This activation is performed in situ under mild conditions (water, room temperature). Isocyanates (R–N=C=O, where R is an alkyl or aryl group) are electrophiles that are highly reactive towards various nucleophiles, including alcohols. Isocyanates form urethane (carbamate) bonds[73] (Fig. 3d and Fig. S2 in the Supplementary Information). However, isocyanates also react with carboxyl groups, releasing CO_2 to form amides and making this strategy non-chemoselective. The use of diisocyanates, which contain two isocyanate moieties, is another strategy to prepare GO-

based frameworks[74]. Alcohols can be deprotonated in the presence of a base, forming alkoxide ions (RO^-), which have a much higher electron density and are thus better nucleophiles than hydroxy functions. Nonetheless, strong bases should be avoided; mild bases, such as potassium carbonate (K_2CO_3), are preferable to avoid the reduction of GO. For instance, the hydroxy groups can be converted to ethers in the presence of alkyl halides (R–X, X = I, Br) and K_2CO_3 (the Williamson reaction; Fig. 3e)[72]. The hydroxy groups can also undergo Michael addition with benzoquinone and react with nitriles under acidic conditions to form esters (the Pinner reaction; see section 1.1 and Fig. S1A,B of the Supplementary Information).

Derivatization of other oxygenated groups

As only a few carboxyl groups are present on the surface of GO (generally in the range 2.5–3.5% of the total oxygenated groups and C=C bonds)[61], derivatization strategies involving these groups lead to low levels of functionalization. The carboxyl groups can react with amines or alcohols in the presence of coupling agents under mild conditions[72,75]. Indeed, amidation and esterification reactions involving the carboxyl groups are extensively used to functionalize GO. However, amidation with amine derivatives is not chemoselective, as epoxides are concurrently opened[61]. Therefore, esterification is the most relevant chemoselective approach (Fig. 2b). The carboxyl groups can also be derivatized through Friedel–Crafts acylation with ferrocene, for example (see section 1.2 and Fig. S1C of the Supplementary Information).

Ketones may also be present in low numbers on the surface of GO, but the reactivity of these groups has not been widely investigated. In one example, the Wittig reaction was studied[72]. However, the reaction was unsuccessful, probably owing to the negligible number of ketones on GO and/or a low reactivity for the Wittig reaction.

Functionalization of C=C bonds

The C=C bonds can also be exploited for the functionalization of GO. The most common strategy involves aryl diazonium salts (ArN_2^+, Ar = aryl), leading to the strong attachment of aryl groups on the GO surface. The diazonium salts are formed from the corresponding anilines, and in the presence of GO they generate highly reactive radicals that add to the C=C bonds[76,77] (Fig. 2c). This reaction is very efficient and compatible with many functional groups. Indeed, the reaction is extensively applied beyond GO for the functionalization of carbon, semiconductors and metals[78],

as well as other types of nanomaterials[79]. The main limitation of this reaction is the risk of oligomerization of the aryl radicals, which can form multilayers or dendritic structures on GO[80]. Other reactions involving the C=C bonds have been reported, such as a Friedel–Crafts-type dithiocarboxylation reaction[81], a Diels–Alder cycloaddition[82] and radical additions[83,84] (see section 1.3 and Fig. S1D,E of the Supplementary Information).

Multifunctionalization

Strategies for the double functionalization of GO can be designed by combining two different reactions. The most efficient approach is based on the opening of the epoxides using nucleophiles, followed by derivatization of the hydroxy groups. Using this approach, high levels of functionalization can be reached, as the two most abundant functional groups are targeted, and epoxide ring opening leads to the formation of additional hydroxy moieties that can participate in the second step. For example, a few studies have reported epoxide opening with various nucleophiles, including amines and thiols, followed by derivatization of the hydroxy groups by etherification, esterification or Michael addition[62,85] (see section 1.4 and Fig. S3 of the Supplementary Information for further details).

Depending on the synthetic protocol, the number of oxygenated groups and defects can vary between batches of GO, which could influence the repeatability of some reactions. Controlling the chemistry of GO is a prerequisite to meeting the requirements of commercial applications, and great effort should be put into standardizing the material[86]. Characterization of derivatized GO samples should focus not only on the type of functional groups grafted on the surface, but also on assessing whether the material is reduced (even partially) during the reaction, such as by X-ray photoelectron spectroscopy (XPS) and thermogravimetric analysis (TGA). For this purpose, performing control reactions under similar conditions, but without a key reagent, may help to determine whether GO is (partially) reduced, providing insight into the outcome of the functionalization. More work should be done to control the degree and type of functionalization, as well as its chemoselectivity.

Characterization of functionalized GO

Careful characterization of any GO-derived material is of utmost importance. As the characterization of GO is complex and can be ambiguous in some cases, it is important to use a combination of different analytical techniques to study the structure and composition of GO after covalent surface modification[87,88]. Table 2 highlights the most important and widely used analytical methods that give structural and chemical information on functionalized GO samples. The main information afforded by each technique is summarized, as well as their strengths and limitations. Several additional complementary analytical techniques are detailed in Table S2 in the Supplementary Information.

Spectroscopy techniques

XPS is a quantitative technique that provides information not only on the elemental composition of GO (except for hydrogen), but also on the nature of the functional groups grafted on its surface, based on peak fitting of the spectral envelopes. However, the deconvolution of the XPS peaks is often complex, ambiguous and may be speculative[88,89] because of the presence of different moieties with similar binding energies. For example, in the case of GO, it is not possible to distinguish between C–OH, ether and epoxide groups. In addition, there are discrepancies in the literature about the position and full width at half maximum values of some functional groups[61,90]. XPS is a surface analysis technique (with an analysis depth of 3–7 nm, depending on the material), but reliable data can be obtained for GO because of its lamellar structure. The characterization of functionalized GO samples by XPS allows one to confirm the presence of elements introduced on the surface of the material, such as nitrogen, sulfur, silicon and halogen atoms[83]. In particular, fluorine atoms are easily detected by XPS, as the F 1*s* core-level transition at 683–694 eV has a high photoionization cross section[62] (Fig. 4a).

NMR spectroscopy is the gold standard technique for assessing the structure of organic substances. But in the case of nanomaterials, their restricted mobility in solution, owing to their large size, and the statistical distribution of the species grafted on their surface contribute to signal broadening[91]. Therefore, NMR spectroscopy in solution is not typically suitable for the characterization of functionalized nanomaterials. Nevertheless, the line broadening can be decreased by rotating a probe containing a solid sample at the magic angle of 54.74° with respect to the direction of the external magnetic field[88]. In this way, magic-angle spinning (MAS) solid-

state NMR has been exploited to characterize GO before and after functionalization[61]. The ^{13}C MAS NMR spectrum of GO contains three main peaks assigned to the epoxides (60-ppm region), C–OH groups (70-ppm region) and C=C bonds (130-ppm region)[24,36]. Quantitative ^{13}C NMR analysis enabled the determination of the relative percentage of all peaks, confirming that the number of carbonyl groups of carboxylic acids and ketones is very low (in the range 2.5–3.5%), depending on the source of GO[61]. In addition, 2D ^{1}H–^{13}C correlation NMR experiments showed that the chemical environment of GO is complex. After reaction with an amine derivative, the relative intensity of the peak attributed to the epoxides in the ^{13}C NMR spectrum was much lower, confirming the occurrence of the epoxide ring-opening reaction[61] (Fig. 4b). Moreover, new peaks arising from molecules grafted on GO can appear. For example, ^{15}N and ^{29}Si MAS NMR were used to confirm the functionalization of GO with azide and silane groups, following reaction with ^{15}N-labelled sodium azide ($Na^{15}N^{14}N_2$)[63] and vinyltrimethoxysilane[92], respectively. Although MAS NMR is a powerful technique, the optimization of some parameters is necessary and complex.

Fourier transform infrared (FTIR) spectroscopy allows for the identification of functional groups grafted on GO by measuring characteristic vibrational modes. The transmission mode using KBr pellets and the attenuated total reflection mode are the two most common FTIR techniques. Owing to the presence of many oxygenated groups, the FTIR spectrum of GO is complex; it is often misinterpreted and some assignments may be speculative. The typical absorption bands observed in the spectrum of GO include a broad and intense band at 3,600–2,400 cm^{-1} (stretching modes of O–H bonds, mainly from water molecules adsorbed on GO, with a minor contribution from tertiary alcohols) and two bands at 1,723 cm^{-1} (stretching mode of C=O bonds, including carboxyl groups, ketones and aldehydes) and 1,619 cm^{-1} (bending modes of water molecules, but often wrongly assigned to stretching modes of C=C bonds)[88,93]. The fingerprint region (500–1,500 cm^{-1}) contains many bands from different functional groups, which are difficult to assign. For example, it is difficult to confirm the derivatization of GO by epoxide ring opening, as the band that could be assigned to the C–O–C vibration of epoxides (at ~1,225–1,250 cm^{-1}) is very small and might be obscured by other bands[61]. The characterization of GO by FTIR spectroscopy has two main drawbacks: first, a lack of sensitivity to detect certain functional groups (some bands can be difficult to distinguish from the background) and second, the risk of an ambiguous assignment of some absorption bands in the fingerprint region. Therefore, only a few bands can be assigned with high confidence. For example, a band at 842 cm^{-1} (S–F stretching) was unambiguously

assigned in the FTIR spectrum of GO functionalized with 3-(pentafluorothio)-phenylalanine[62]. The absorption bands appearing in the region 2,100–2,300 cm^{-1} are characteristic of the stretching vibrations of nitriles (–C≡N; 2,194 cm^{-1})[65], isocyanates (2,277 cm^{-1})[74] and azide groups (2,122–2,123 cm^{-1})[63,94] (Fig. 4c). Another example is the appearance of bands characteristic of Si–O–C (1,016 cm^{-1}) and Si–O–Si bonds (1,109 cm^{-1}) in the FTIR spectrum of GO functionalized by silanization[92].

The Raman spectrum of graphite displays two main peaks: the G band at ~1,580 cm^{-1}, corresponding to planar vibrations of the carbon atoms, and the D band at ~1,350 cm^{-1}, related to structural defects. In the Raman spectrum of GO, the G band is broadened and the D band intensity (I_D) increases and can be higher than the G band intensity (I_G), as a result of the structural disorder in the sp^2 domain. The functionalization of the oxygenated groups of GO does not lead to notable changes in the Raman spectrum. By contrast, radical addition to the C=C bonds can result in a slightly higher I_D/I_G ratio, owing to the rehybridization of some sp^2 carbon atoms to sp^3 (refs[76,83]) (Fig. 4d). If the molecules grafted on GO are Raman-active, specific bands can appear, as in the case of C_{60} (ref.[95]). When GO is derivatized with an electron-acceptor or electron-donor molecule, a shift is observed in the G band, which is indicative of molecular charge transfer. Such a shift was observed in the Raman spectrum of ferrocene-functionalized GO[96]. An advanced Raman technique, tip-enhanced Raman spectroscopy, enables surface molecular mapping of materials with a high chemical sensitivity and spatial resolution (~10 nm). This method was used to visualize the distribution of the structural defects and the different oxygenated groups of GO derivatized with carboxyl groups[97].

Ultraviolet–visible (UV–vis) spectroscopy can be used to measure the optical absorption of GO and to detect the specific absorption of molecules conjugated on its surface, such as anthracene[98] or polymers[99]. The UV–vis spectrum of GO displays two characteristic peaks: a maximum absorption at ~231 nm and a shoulder at ~300 nm, which are assigned to the π–π* transition of aromatic C=C bonds and to the *n*–π* transition of C=O bonds, respectively[87].

Thermal analysis

Thermogravimetric analysis is a technique used to assess the thermal stability of materials by measuring the weight loss of a sample as a function of increasing temperature in an inert atmosphere or air. The TGA profile of GO in nitrogen or argon gas exhibits three main steps[61]. GO

is thermally unstable and starts to lose weight at temperatures below 100 °C, mainly due to the removal of adsorbed water. The main weight-loss step occurs at ~200 °C and is attributed to the decomposition of the most labile oxygenated groups. A slow and steady decrease in weight is observed above 250 °C and is ascribed to the removal of more stable oxygenated functional groups. TGA can be useful in determining the level of functionalization of GO by estimating the concentration of organic molecules attached to the surface. TGA can also be coupled with mass spectrometry (MS) or FTIR to help identify the desorbed species. As an example, TGA-MS was able to detect labelled nitrogen gas ($^{15}N^{14}N$) released from GO functionalized with ^{15}N-labelled sodium azide[63] (Fig. 4e). Nevertheless, the interpretation of TGA data is generally difficult for several reasons. First, because GO is thermally unstable, it is necessary to analyse control samples, prepared by treating GO under similar conditions as those of the reaction but without one key reagent, for accurate comparison[61]. Indeed, mild heating can lead to the removal of some labile groups from the surface of GO during functionalization reactions, which can result in unwanted changes in the composition, for example. The comparison with control samples allows one to establish whether differences in the TGA curves are due to the functionalization or due to loss of other groups during functionalization. Second, when the molecules grafted on GO have a low molecular weight, it is difficult to see significant differences in weight loss for GO samples before and after functionalization. TGA is therefore more useful when GO is derivatized with high-molecular-weight molecules. Finally, there can be some variations between analyses, and the TGA curves may not coincide perfectly for samples from a single batch, mainly because GO samples are not homogeneous and uniform. To overcome this reproducibility issue, TGA measurements have to be performed on at least three aliquots from the same batch to obtain analyses that are as accurate as possible.

Microscopy techniques

Transmission electron microscopy (TEM) and scanning electron microscopy (SEM) can be used to verify that the morphology of GO sheets has not been affected by chemical treatments. Electron microscopy images of GO typically show wrinkled and folded 2D sheets with a rough surface and irregular edges in some cases. High-resolution TEM enables the visualization of the characteristic hexagonal lattices in graphene sheets[100]. In the case of C_{60} grafted onto GO, the fullerene moieties appear as individual spherical structures with an inner diameter of ~0.7 nm (ref.[95]) (Fig. 4f).

Electron microscopes can be equipped with an energy-dispersive X-ray (EDX) analyser, which enables the identification of the elemental composition of the surface of functionalized GO[101]. Used in conjunction with electron microscopy, electron energy-loss spectroscopy (EELS) can also measure the elemental composition of GO by measuring the energy lost by incident electrons after interacting with the material. Both EELS and EDX can determine the spatial distribution of elements on GO through mapping[81]. EELS is more appropriate for detecting the elements ranging from carbon to the 3*d* transition metals, whereas EDX is particularly sensitive to heavier elements. The main difference between EDX analysis and EELS is the difference in energy resolution (<130 eV and <2 eV, respectively), with the higher resolution of EELS allowing one to assess the different forms of the same element. Nevertheless, the sensitivity of GO to high-energy electron irradiation can limit the use of EELS for the study of GO. By decreasing the electron illumination below the damage limit through optimization of the acquisition conditions and the experimental setup, a spatial resolution of 3 nm was obtained, enabling the assessment of the spatial distribution of oxygen on GO; this approach could also be applied to functionalized GO[102].

Atomic force microscopy (AFM) is a type of high-resolution scanning probe microscopy that is employed to provide 3D information on the surface topology of materials at the nanometre scale. This technique gives information on the thickness of the GO flakes and their lateral size. Owing to the presence of the oxygenated groups, the interlayer distance between GO sheets is greater than that between two layers of graphene and varies from 0.9 to 1.3 nm, because of adsorbed water molecules on the surface of GO and also depending on the measurement conditions[103]. An increased thickness is observed after functionalization of GO with large molecules (such as polymers)[104]. AFM can be coupled with infrared (IR) spectroscopy to overcome the limitations associated with IR diffraction limits. This technique enables IR spectroscopy to be performed at AFM resolution, and it can be used to chemically map a sample by coupling the IR spectra of specific areas to information on the topography. Applied to the characterization of GO, AFM-IR identified the location of oxygen atoms and also the type of bonding with a nanometre spatial resolution[105]. The use of such techniques to characterize functionalized GO opens the possibility of establishing a link between the nanoscale structure and composition, and the properties and function of the material.

Other analytical methods

Elemental analysis can be performed to accurately assess the elemental composition of GO samples[61,63,81]. Different techniques can be used, including combustion and inductively coupled plasma atomic emission spectroscopy.

X-ray diffraction (XRD) can give information on the interlayer distance (*d*-spacing) of GO by measuring the intensity of scattered X-rays as a function of scattering angle. Using this technique, it is possible to estimate the degree of exfoliation and also the impact of functionalization with relatively large molecules on the interlayer distance of GO. For instance, the *d*-spacing increased after grafting benzenesulfonic groups onto GO[76]. In another study, the interlayer spacing between GO layers was dependent on the length of boronic acid derivatives grafted on the diol moieties[69], and the surface area increased as a function of interlayer spacing. Indeed, the surface area of GO functionalized with boronic acid, measured through the sorption of nitrogen gas at 77 K and based on Brunauer–Emmett–Teller (BET) theory, was much higher than that of bare GO.

Assessment of the zeta potential provides a measure of the effective electric charge on the surface of GO. Because of the presence of numerous oxygenated groups, GO has a highly negative zeta potential (generally between approximately –45 and –50 mV). Functionalization can affect the surface charge of the material, depending on the chemical strategy and the type of grafted species, namely whether they are neutral or positively or negatively charged. For example, after functionalization of GO with isophorone diisocyanate, which is a neutral molecule, the zeta potential increased from –42.1 to –15.8 mV at pH 7 (ref.[76]). By contrast, the value was slightly more negative (changing from –39.3 to –42.2 mV) after grafting benzenesulfonic acid by arylation to the C=C bonds[76].

Other techniques can be used to characterize the properties of specific molecules conjugated to GO. For example, cyclic voltammetry can be used to study the electrochemical properties of molecules grafted on GO, such as benzoquinone. In this case, the characteristic oxidation and reduction potentials of benzoquinone were observed for the GO–benzoquinone conjugate[62]. In another study, the presence of C_{60} on GO was confirmed by analysing the electrochemical redox behaviour of a covalent GO–C_{60} hybrid[95]. The slight shift in the reduction potential could be indicative of interactions between GO and the fullerene derivative.

Applications of functionalized graphene oxide

GO has been exploited for various applications in different fields, from sensing, catalysis and composites to environmental science, energy and biomedicine[15,106-109]. The chemical composition of GO influences its properties, and the covalent grafting of molecules on its surface represents a valuable strategy to modulate and enhance the material performance for different applications. In this section, we describe examples of the use of functionalized GO in the areas in which they find most applications — namely environmental- and energy-related areas — focusing on studies in which GO was functionalized under mild conditions and with high chemoselectivity. In the Supplementary Information (Section 3), we also provide an overview of their biomedical applications.

Environmental applications

In a bid to increase sustainability and energy efficiency, GO has been investigated for environmental applications in drinking water purification; membrane separation processes, including water desalination; and osmotic energy harvesting[9,110]. The function and performance of GO-based materials in environmental applications, and particularly for the development of separation membranes, is governed not only by the chemistry of GO, but also by its hierarchical structure. Separation membranes made of GO consist of horizontally aligned GO flakes and nanoplatelets, stacked in a lamellar structure that is stable in water[111] (Fig. 5a,b). Once hydrated, the membrane swells[112,113], with the nature of the functional groups determining the interlayer distance between the flakes. As the solution penetrates between the flakes, it flows along the GO basal plane in a percolative path between segregated functional groups[114], until it serpentines across the membrane[115]. The frictionless surface of pristine graphene regions facilitates ultrafast water transport[12]. The selectivity of the membranes is based on the size exclusion[116] and dehydration[117,118] of hydrated ions (determined by the interlayer distance), charge selectivity[117] (through protonizable functional groups) and chemical affinity[119]. For the well-established technology of pressure-driven desalination (reverse osmosis), GO membranes are yet to reach the performance of traditional thin-film composite membranes[120], largely owing to the inferior ion/water selectivity of GO. Attempts to decrease the interlayer distance between GO flakes by physical constraints[117] and chemical crosslinking[121] did not notably improve the reverse osmosis performance. However, owing to their high charge selectivity, GO membranes could yet have an edge in two emerging technologies[118,122]:

electrodialysis desalination and energy harvesting by reverse electrodialysis[122]. The other prominent applications for GO membranes are organic solvent separation[123] and pervaporation[124], which is a membrane evaporation process for the separation of organic–water and organic–organic mixtures.

GO can also be assembled into sponge and related 3D forms[125,126], in which their high surface area facilitates the adsorption of contaminants (Fig. 5c). Compared with traditional adsorbent materials, such as porous carbon-based materials, bioadsorbents and zeolites, GO has a higher adsorption capacity for heavy metals owing to the high density of ion-chelating anionic functional groups. The specificity for certain contaminants is determined by the chemical modification of the GO surface, which promote electrostatic and π–π interactions between GO and the contaminants. A notable application of GO sorbents is in the purification of drinking water through the removal of low concentrations of harmful contaminants, including dyes[74], organics[127], drugs[128] and heavy metals[74,129,130].

The functionalization of GO can enhance its adsorption capacity. For example, GO-framework membranes were fabricated by crosslinking GO sheets using isophorone diisocyanate for the removal of dyes and heavy metals[74]. Crosslinking increased the structural stability of the membranes as well as the water permeability. In another example, GO was modified by silanization with a silane functionalized with a cheating agent (ethylenediamine triacetic acid) to increase its adsorption capacity for the removal of heavy metals[129,130]. In the case of polymeric membranes, the functionalization of GO can be necessary to prevent aggregation of the sheets. Using this strategy, the hydroxy groups of GO were derivatized by esterification using hydroxylated sulfonated poly(ether ether ketone) (SPEEK) and incorporated into polysulfone to prepare a membrane for the removal of natural organic matter[127]. The membranes displayed tunable porosity and high water flux.

GO has remarkable antimicrobial properties, mainly because of its sharp edges, which can cause physical damage to bacterial membranes, leading to their structural destruction[130-133]. Thus, GO sorbents are attractive options for point-of-use water treatment. With large pore sizes and high levels of chemical reduction, GO sponges attain a very high capacity for the adsorption of hydrocarbons[134], becoming a prospective solution for the removal of oil and organic solvents in freshwater and marine environments.

Energy applications

Because of the increasing energy demand, fuel cells have attracted considerable interest, as they are an environmentally friendly and efficient alternative energy source for many applications[135-137]. There is a plethora of articles on the use of functionalized GO for energy-related applications[15,138,139]. Here, we highlight a few examples in which the functionalization of GO was well controlled. Proton-exchange membrane (PEM) fuel cells, which are generally made from polyelectrolytes, convert chemical energy into electrical energy through an electrochemical reaction between hydrogen and oxygen gas with the concomitant generation of water and heat[140]. The performance of PEMs strongly depends on their proton transport capacity, and thus considerable research efforts are invested in developing PEMs with high proton conductivity. In this regard, there are two main approaches: the modification of existing polyelectrolytes and PEMs with additives, or the synthesis of new polyelectrolytes for the design of novel PEMs. As an example, GO functionalized thorugh an atom-transfer radical addition reaction with Nafion was used as an additive in the fabrication of Nafion-based composite PEMs for fuel cells. Compared with a Nafion membrane, the composite exhibited a higher proton conductivity[83]. The improved performance was attributed to the aggregation of the sulfonic acid groups of the Nafion chains grafted onto GO, which form proton-conducting domains. Nevertheless, the high cost of Nafion membranes and decreased proton conductivity above 80 °C limit the large-scale application and wide-spread commercialization of fuel cells, and much effort is being devoted to the development of new and cheaper materials.

Owing to its large surface area and the abundance of oxygenated groups, GO can be used as an inorganic filler in polymer electrolyte membranes. The incorporation of GO enhances both the transport of protons and the uptake of water in the membranes, while providing mechanical stability and an electron-insulating environment[141-143]. The presence of other acidic groups on GO, in addition to the oxygenated functional groups, can provide a better network for proton transport. In this regard, the functionalization of GO with sulfonic acid groups, such as by derivatization of the hydroxy groups with chlorosulfonic acid or by arylation of the C=C bonds using the diazonium salt of aniline-4-sulfonic acid, has been extensively investigated[144]. As an example, GO functionalized with sulfonic acid by arylation was incorporated into a SPEEK matrix. The composite membrane displayed a higher proton conductivity and superior fuel cell performance than did SPEEK[145] (Fig. 5d). For such applications, the retention of the oxygenated groups during the chemical

functionalization of GO is essential to retain the intrinsic high proton conductivity and water-retention properties.

Conclusions and perspectives

The relatively low-cost production of GO and its dispersibility in various solvents, including water, combined with its tunable surface chemistry, make GO an attractive building block for multifunctional materials. There are many applications for which it is fundamental to preserve the intrinsic properties of GO. For instance, the high density of oxygenated groups in GO leads to a high water dispersibility (important in biomedicine) and to a high proton conductivity and water retention (relevant for fuel cell applications). As a consequence, the derivatization of GO to impart new properties has to be well controlled and the functionalized samples thoroughly characterized. These tasks are complex, because the chemical structure of GO has not been fully elucidated and it can vary in terms of the ratio of different oxygenated groups, and the level of defects, depending on the synthesis protocol and the graphite source. All structural models converge on the fact that the basal plane of GO contains abundant epoxide and hydroxy groups, which can be exploited for functionalization to tailor the properties of the material, whereas carboxyl groups are present only in low numbers. Despite the great progress in the functionalization of GO, the chemistry of GO is not always well controlled and not fully understood.

The chemical structure of functionalized GO reported in the literature is sometimes incomplete or incorrect, mainly because the side reactions have not been taken into account. The reactivity of GO is determined by a complex set of factors, as the oxygenated groups reside in a rich and unusual chemical environment, and notable in-plane distortions and strain in the lattice can increase their reactivity. With different oxygenated groups on the surface of GO and the high chemical reactivity of some reagents, simultaneous reactions may occur, yielding uncontrolled GO derivatives.

The main goal of this Review is to clarify the chemical reactivity of GO and give critical and useful advice on how to facilitate its functionalization without reduction of the material, which would affect its properties. We have emphasized the importance of chemoselective reactions, which allow one to derivatize a specific oxygenated group or the C=C bonds without affecting the other moieties, thus providing possibilities for controlled multifunctionalization of GO. The easiest

and most efficient strategies involve the epoxide and hydroxy groups, because they are present in large numbers.

When functionalizing GO, it is important to use mild reaction conditions, in particular in terms of temperature and pH when needed, to avoid the removal of labile oxygenated groups and the degradation of the GO framework. In this Review, we have mostly described reactions that do not require thermal activation and are performed at room temperature. Substantial reduction of GO can generally be prevented when reactions are performed below 80 °C. Nevertheless, some studies report rather harsh conditions for GO functionalization, even though they are not needed.

Post-reaction characterization of the type and number of functional groups introduced after derivatization is a crucial yet difficult task owing to the heterogeneous structure of GO. Even more complex is the confirmation of the successful outcome of covalent chemoselective functionalization. By means of different techniques, including TGA, XPS and solid-state NMR, complementary information can be obtained, but it is hard to get conclusive and unambiguous data. The use of molecules that contain labelled elements or functional groups that are easily detectable by certain techniques, such as FTIR or XPS, can facilitate characterization.

Although considerable effort has been devoted to the study of GO, further investigations are needed to understand the relationship between the physicochemical structure and the properties of the material. A crucial question is how functionalization affects its global properties. In addition, examination of the long-term stability of functionalized GO is imperative from a commercial perspective. More knowledge about the chemical structure of GO is essential to clarify the changes that occur after functionalization. In this regard, collaboration between chemists, material scientists and physicists will help to overcome the issues related to the unique and not fully explored reactivity of GO and its characterization to achieve controlled functionalization and extend the field of research and applications of GO-based materials.

Acknowledgements

The authors gratefully acknowledge the support of the Centre National de la Recherche Scientifique (CNRS) and the International Center for Frontier Research in Chemistry (icFRC), as well as financial support from the Agence Nationale de la Recherche (ANR) through the Interdisciplinary Thematic Institute ITI-CSC via the IdEx Unistra (ANR-10-IDEX-0002) within the programme ‘Investissement d’Avenir’ and from the European Commission through the

Graphene Flagship Core 3 project (award no. 881603). S. Garaj acknowledges support from the National Research Foundation, Prime Minister's Office, Singapore, under the Competitive Research Program (award no. NRF-CRP13-2014-03), and from the Agency for Science, Technology and Research (A*STAR), Singapore, under its Advanced Manufacturing and Engineering (AME) Programmatic grant (award no. A18A9b0060). S. Guo is indebted to the Chinese Scholarship Council for supporting his PhD internship.

Author contributions

C.M.-M. conceptualized the manuscript. S. Guo, S. Garaj and C.M.-M. wrote the initial draft. All authors edited the manuscript prior to submission.

Competing interests

The authors declare no competing interests.

Supplementary information

Supplementary information is available for this paper at https://doi.org/10.1038/s42254-022-00422- w

References

1. Novoselov, K. S. *et al.* Electric field effect in atomically thin carbon films. *Science* **306**, 666–669 (2004).

2. Konios, D., Stylianakis, M. M., Stratakis, E. & Kymakis, E. Dispersion behaviour of graphene oxide and reduced graphene oxide. *J. Colloid Interface Sci.* **430**, 108–112 (2014).

3. Clancy, A. J., Au, H., Rubio, N., Coulter, G. O. & Shaffer, M. S. P. Understanding and controlling the covalent functionalisation of graphene. *Dalton Trans.* **49**, 10308–10318 (2020).

4. Brisebois, P. P. & Siaj, M. Harvesting graphene oxide – years 1859 to 2019: a review of its structure, synthesis, properties and exfoliation. *J. Mater. Chem. C* **8**, 1517–1547 (2020).

This review gives a comprehensive overview of the synthetic methods used to prepare GO and details its molecular structure.

5. Johari, P. & Shenoy, V. B. Modulating optical properties of graphene oxide: role of prominent functional groups. *ACS Nano* **5**, 7640–7647 (2011).

6. Lin, S. & Buehler, M. J. Thermal transport in monolayer graphene oxide: atomistic insights into phonon engineering through surface chemistry. *Carbon* **77**, 351–359 (2014).
7. Mei, Q. *et al.* Graphene oxide: from tunable structures to diverse luminescence behaviors. *Adv. Sci.* **6**, 1900855 (2019).
8. Huang, Y. *et al.* Graphene oxide assemblies for sustainable clean-water harvesting and green-electricity generation. *Acc. Mater. Res.* **2**, 97–107 (2021).
9. Li, F., Jiang, X., Zhao, J. & Zhang, S. Graphene oxide: a promising nanomaterial for energy and environmental applications. *Nano Energy* **16**, 488–515 (2015).
10. Kim, F., Cote, L. J. & Huang, J. Graphene oxide: surface activity and two-dimensional assembly. *Adv. Mater.* **22**, 1954–1958 (2010).
11. Ménard-Moyon, C., Bianco, A. & Kalantar-Zadeh, K. Two-dimensional material-based biosensors for virus detection. *ACS Sens.* **5**, 3739–3769 (2020).
12. Nair, R. R., Wu, H. A., Jayaram, P. N., Grigorieva, I. V. & Geim, A. K. Unimpeded permeation of water through helium-leak–tight graphene-based membranes. *Science* **335**, 442–444 (2012).
13. Lombardi, L. & Bandini, M. Graphene oxide as a mediator in organic synthesis: a mechanistic focus. *Angew. Chem. Int. Ed.* **59**, 20767–20778 (2020).
14. Soltani, R., Guo, S., Bianco, A. & Ménard-Moyon, C. Carbon nanomaterials applied for the treatment of inflammatory diseases: preclinical evidence. *Adv. Therap.* **3**, 2000051 (2020).
15. Georgakilas, V. *et al.* Noncovalent functionalization of graphene and graphene oxide for energy materials, biosensing, catalytic, and biomedical applications. *Chem. Rev.* **116**, 5464–5519 (2016).
16. Hummers, W. S. & Offeman, R. E. Preparation of graphitic oxide. *J. Am. Chem. Soc.* **80**, 1339–1339 (1958).
17. Nishina, Y. & Eigler, S. Chemical and electrochemical synthesis of graphene oxide – a generalized view. *Nanoscale* **12**, 12731–12740 (2020).
This review summarizes the recent progress made in the controlled synthesis of GO.
18. Zhang, Q. *et al.* The realistic domain structure of as-synthesized graphene oxide from ultrafast spectroscopy. *J. Am. Chem. Soc.* **135**, 12468–12474 (2013).
19. Chouhan, A., Mungse, H. P. & Khatri, O. P. Surface chemistry of graphene and graphene oxide: a versatile route for their dispersion and tribological applications. *Adv. Colloid Interface Sci.* **283**, 102215 (2020).

20. Motevalli, B., Parker, A. J., Sun, B. & Barnard, A. S. The representative structure of graphene oxide nanoflakes from machine learning. *Nano Futures* **3**, 045001 (2019).

21. He, H., Klinowski, J., Forster, M. & Lerf, A. A new structural model for graphite oxide. *Chem. Phys. Lett.* **287**, 53–56 (1998).

22. Casabianca, L. B. *et al.* NMR-based structural modeling of graphite oxide using multidimensional ^{13}C solid-state NMR and ab initio chemical shift calculations. *J. Am. Chem. Soc.* **132**, 5672–5676 (2010).

23. De Jesus, L. R. *et al.* Inside and outside: X-ray absorption spectroscopy mapping of chemical domains in graphene oxide. *J. Phys. Chem. Lett.* **4**, 3144–3151 (2013).

24. Gao, W., Alemany, L. B., Ci, L. & Ajayan, P. M. New insights into the structure and reduction of graphite oxide. *Nat. Chem.* **1**, 403–408 (2009).

25. Erickson, K. *et al.* Determination of the local chemical structure of graphene oxide and reduced graphene oxide. *Adv. Mater.* **22**, 4467–4472 (2010).

This work uses ultra-high-resolution TEM to reveal the local atomic structure of GO.

26. Aliyev, E. *et al.* Structural characterization of graphene oxide: surface functional groups and fractionated oxidative debris. *Nanomaterials* **9**, 1180 (2019).

27. Eigler, S., Dotzer, C. & Hirsch, A. Visualization of defect densities in reduced graphene oxide. *Carbon* **50**, 3666–3673 (2012).

28. Feicht, P. & Eigler, S. Defects in graphene oxide as structural motifs. *ChemNanoMat* **4**, 244–252 (2018).

29. Dimiev, A., Kosynkin, D. V., Alemany, L. B., Chaguine, P. & Tour, J. M. Pristine graphite oxide. *J. Am. Chem. Soc.* **134**, 2815–2822 (2012).

This work proposes a mechanism for the reaction of GO with water.

30. Eigler, S., Dotzer, C., Hof, F., Bauer, W. & Hirsch, A. Sulfur species in graphene oxide. *Chem. Eur. J.* **19**, 9490–9496 (2013).

31. Dimiev, A. M. in *Graphene oxide: fundamentals and applications* Ch. 2 (eds Dimiev, A. M. & Eigler, S.) (Wiley, 2017).

32. Yang, L. *et al.* π-Conjugated carbon radicals at graphene oxide to initiate ultrastrong chemiluminescence. *Angew. Chem. Int. Ed.* **53**, 10109–10113 (2014).

33. Hou, X.-L. *et al.* Tuning radical species in graphene oxide in aqueous solution by photoirradiation. *J. Phys. Chem. C* **117**, 6788–6793 (2013).

34. Pieper, H. *et al.* Endoperoxides revealed as origin of the toxicity of graphene oxide. *Angew. Chem. Int. Ed.* **55**, 405–407 (2016).
35. Shin, D. S. *et al.* Distribution of oxygen functional groups of graphene oxide obtained from low-temperature atomic layer deposition of titanium oxide. *RSC Adv.* **7**, 13979–13984 (2017).
36. Lerf, A., He, H., Forster, M. & Klinowski, J. Structure of graphite oxide revisited. *J. Phys. Chem. B* **102**, 4477–4482 (1998).
37. Szabó, T. *et al.* Evolution of surface functional groups in a series of progressively oxidized graphite oxides. *Chem. Mater.* **18**, 2740–2749 (2006).
38. Chua, C. K., Sofer, Z. & Pumera, M. Graphite oxides: effects of permanganate and chlorate oxidants on the oxygen composition. *Chem. Eur. J.* **18**, 13453–13459 (2012).
39. Feicht, P. *et al.* Brodie's or Hummers' method: oxidation conditions determine the structure of graphene oxide. *Chem. Eur. J.* **25**, 8955–8959 (2019).
40. Chen, Z.-L. *et al.* Influence of graphite source on chemical oxidative reactivity. *Chem. Mater.* **25**, 2944–2949 (2013).
41. Mkhoyan, K. A. *et al.* Atomic and electronic structure of graphene-oxide. *Nano Lett.* **9**, 1058–1063 (2009).
42. Komeily-Nia, Z., Qu, L.-T. & Li, J.-L. Progress in the understanding and applications of the intrinsic reactivity of graphene-based materials. *Small Sci.* **1**, 2000026 (2021).
43. Bissett, M. A., Konabe, S., Okada, S., Tsuji, M. & Ago, H. Enhanced chemical reactivity of graphene induced by mechanical strain. *ACS Nano*. **7**, 10335–10343 (2013).
44. Xin, G. *et al.* Tunable photoluminescence of graphene oxide from near-ultraviolet to blue. *Mater. Lett.* **74**, 71–73 (2012).
45. Rourke, J. P. *et al.* The real graphene oxide revealed: stripping the oxidative debris from the graphene-like sheets. *Angew. Chem. Int. Ed.* **50**, 3173–3177 (2011).
46. Thomas, H. R. *et al.* Deoxygenation of graphene oxide: reduction or cleaning? *Chem. Mater.* **25**, 3580–3588 (2013).
47. Naumov, A. *et al.* Graphene oxide: a one- versus two-component material. *J. Am. Chem. Soc.* **138**, 11445–11448 (2016).
48. Rourke, J. P. & Wilson, N. R. Letter to the editor: a defence of the two-component model of graphene oxide. *Carbon* **96**, 339–341 (2016).

49. Gudarzi, M. M. Colloidal stability of graphene oxide: aggregation in two dimensions. *Langmuir* **32**, 5058–5068 (2016).

50. Whitby, R. L. D. *et al.* Driving forces of conformational changes in single-layer graphene oxide. *ACS Nano* **6**, 3967–3973 (2012).

51. Du, W., Wu, H., Chen, H., Xu, G. & Li, C. Graphene oxide in aqueous and nonaqueous media: dispersion behaviour and solution chemistry. *Carbon* **158**, 568–579 (2020).

52. Dimiev, A. M., Alemany, L. B. & Tour, J. M. Graphene oxide. Origin of acidity, its instability in water, and a new dynamic structural model. *ACS Nano* **7**, 576–588 (2013).

Complementary to Dimiev, A et al. *J. Am. Chem. Soc.* 134, 2815–2822 (2012), this article includes a reaction scheme that illustrates the transformation of GO caused by reaction with water.

53. Chua, C. K. & Pumera, M. Graphene oxide: light and atmosphere affect the quasi-equilibrium states of graphite oxide and graphene oxide powders. *Small* **11**, 1266–1272 (2015).

54. Taniguchi, T. *et al.* pH-driven, reversible epoxy ring opening/closing in graphene oxide. *Carbon* **84**, 560–566 (2015).

55. Eigler, S., Grimm, S., Hof, F. & Hirsch, A. Graphene oxide: a stable carbon framework for functionalization. *J. Mater. Chem. A* **1**, 11559–11562 (2013).

56. Fan, X. *et al.* Deoxygenation of exfoliated graphite oxide under alkaline conditions: a green route to graphene preparation. *Adv. Mater.* **20**, 4490–4493 (2008).

57. Dimiev, A. M. & Polson, T. A. Contesting the two-component structural model of graphene oxide and reexamining the chemistry of graphene oxide in basic media. *Carbon* **93**, 544–554 (2015).

58. Chen, C., Kong, W., Duan, H. M. & Zhang, J. Theoretical simulation of reduction mechanism of graphene oxide in sodium hydroxide solution. *Phys. Chem. Chem. Phys.*, **16**, 12858–12864 (2014).

59. Kumar, P. V. *et al.* Scalable enhancement of graphene oxide properties by thermally driven phase transformation. *Nat. Chem.* **6**, 151–158 (2014).

60. Eigler, S., Dotzer, C., Hirsch, A., Enzelberger, M. & Müller, P. Formation and decomposition of CO_2 intercalated graphene oxide. *Chem. Mater.* **24**, 1276–1282 (2012).

61. Vacchi, I. A., Spinato, C., Raya, J., Bianco, A. & Ménard-Moyon, C. Chemical reactivity of graphene oxide towards amines elucidated by solid-state NMR. *Nanoscale* **8**, 13714–13721 (2016).

This study elucidates the reactivity of GO towards amine derivatives (epoxide ring opening) and the low content of carboxylic acids at the edges.

62. Guo, S., Nishina, Y., Bianco, A. & Ménard-Moyon, C. A flexible method for covalent double functionalization of graphene oxide. *Angew. Chem. Int. Ed.* **59**, 1542–1547 (2020).

63. Eigler, S., Hu, Y., Ishii, Y. & Hirsch, A. Controlled functionalization of graphene oxide with sodium azide. *Nanoscale* **5**, 12136–12139 (2013).

64. Mei, K.-C. *et al.* Synthesis of double-clickable functionalised graphene oxide for biological applications. *Chem. Commun.* **51**, 14981–14984 (2015).

65. Collins, W. R., Schmois, E. & Swager, T. M. Graphene oxide as an electrophile for carbon nucleophiles. *Chem. Commun.* **47**, 8790–8792 (2011).

66. Liu, Y. *et al.* Enhancement of proton conductivity of chitosan membrane enabled by sulfonated graphene oxide under both hydrated and anhydrous conditions. *J. Power Sources* **269**, 898–911 (2014).

67. Mondal, S., Papiya, F., Ash, S. N. & Kundu, P. P. Composite membrane of sulfonated polybenzimidazole and sulfonated graphene oxide for potential application in microbial fuel cell. *J. Environ. Chem. Eng.* **9**, 104945 (2021).

68. Gao, T., Wu, H., Tao, L., Qu, L. & Li, C. Enhanced stability and separation efficiency of graphene oxide membranes in organic solvent nanofiltration. *J. Mater. Chem. A* **6**, 19563–19569 (2018).

69. Srinivas, G., Burress, J. W., Ford, J. & Yildirim, T. Porous graphene oxide frameworks: synthesis and gas sorption properties. *J. Mater. Chem.* **21**, 11323–11329 (2011).

70. Pourazadi, E., Haque, E., Zhang, W., Harris, A. T. & Minett, A. I. Synergistically enhanced electrochemical (ORR) activity of graphene oxide using boronic acid as an interlayer spacer. *Chem. Commun.* **49**, 11068–11070 (2013).

71. Sun, J. *et al.* A molecular pillar approach to grow vertical covalent organic framework nanosheets on graphene: hybrid materials for energy storage. *Angew. Chem. Int. Ed.* **57**, 1034–1038 (2018).

72. Vacchi, I. A., Raya, J., Bianco, A. & Ménard-Moyon, C. Controlled derivatization of hydroxyl groups of graphene oxide in mild conditions. *2D Mater.* **5**, 035037 (2018).

73. Stankovich, S., Piner, R. D., Nguyen, S. T. & Ruoff, R. S. Synthesis and exfoliation of isocyanate-treated graphene oxide nanoplatelets. *Carbon* **44**, 3342–3347 (2006).

74. Zhang, P. *et al.* Cross-linking to prepare composite graphene oxide-framework membranes with high-flux for dyes and heavy metal ions removal. *Chem. Eng. J.* **322**, 657–666 (2017).
75. Song, W. *et al.* Synthesis and nonlinear optical properties of reduced graphene oxide hybrid material covalently functionalized with zinc phthalocyanine. *Carbon* **77**, 1020–1030 (2014).
76. Tang, L., Lu, Y., Yao, L. & Cui, P. A highly hydrophilic benzenesulfonic-grafted graphene oxide-based hybrid membrane for ethanol dehydration. *RSC Adv.* **10**, 20358–20367 (2020).
77. Shen, J. et al. Upper-critical solution temperature (UCST) polymer functionalized graphene oxide as thermally responsive ion permeable membrane for energy storage devices. *J. Mater. Chem. A* **2**, 18204–18207 (2014).
78. Pinson, J. & Podvorica, F. Attachment of organic layers to conductive or semiconductive surfaces by reduction of diazonium salts. *Chem. Soc. Rev.* **34**, 429–439 (2005).
79. Li, D. *et al.* Surface functionalization of nanomaterials by aryl diazonium salts for biomedical sciences. *Adv. Colloid Interface Sci.* **294**, 102479 (2021).
80. Hossain, Md. Z., Walsh, M. A. & Hersam, M. C. Scanning tunneling microscopy, spectroscopy, and nanolithography of epitaxial graphene chemically modified with aryl moieties. *J. Am. Chem. Soc.* **132**, 15399–15403 (2010).
81. Jankovský, O. *et al.* Introduction of sulfur to graphene oxide by Friedel-Crafts reaction. *FlatChem* **6**, 28–36 (2017).
82. Brisebois, P. P., Kuss, C., Schougaard, S. B., Izquierdo, R. & Siaj, M. New insights into the Diels–Alder reaction of graphene oxide. Chem. Eur. J. 22, 5849–5852 (2016).
83. Peng, K.-J., Lai, J.-Y. & Liu, Y.-L. Nanohybrids of graphene oxide chemically-bonded with Nafion: preparation and application for proton exchange membrane fuel cells. *J. Membr. Sci.* **514**, 86–94 (2016).
84. Peng, K.-J., Wang, K.-H., Hsu, K.-Y. & Liu, Y.-L. Building up polymer architectures on graphene oxide sheet surfaces through sequential atom transfer radical polymerization. *J. Polym. Sci., Part A: Polym. Chem.* **52**, 1588–1596 (2014).
85. Vacchi, I. A., Guo, S., Raya, J., Bianco, A. & Ménard-Moyon, C. Strategies for the controlled covalent double functionalization of graphene oxide. *Chem. Eur. J.* **26**, 6591–6598 (2020).
86. Amadei, C. A., Arribas, P. & Vecitis, C. D. Graphene oxide standardization and classification: methods to support the leap from lab to industry. *Carbon* **133**, 398–409 (2018).

87. Zhang, Z., Schniepp, H. C. & Adamson, D. H. Characterization of graphene oxide: variations in reported approaches. *Carbon* **154**, 510–521 (2019).

This review highlights the consistencies and inconsistencies of the techniques used to characterize GO.

88. Dimiev, A. M. & Eigler, S. in *Graphene oxide: fundamentals and applications* (eds Dimiev, A. M. & Eigler, S.) Ch. 3 (Wiley, 2017).

89. Kovtun, A. *et al.* Accurate chemical analysis of oxygenated graphene-based materials using X-ray photoelectron spectroscopy. *Carbon* **143**, 268–275 (2019).

90. Greczynski, G. & Hultman, L. Compromising science by ignorant instrument calibration—need to revisit half a century of published XPS data. *Angew. Chem. Int. Ed.* **59**, 5002–5006 (2020).

91. Deng, Y., Li, Y., Dai, J., Lang, M. & Huang, X. Functionalization of graphene oxide towards thermo-sensitive nanocomposites via moderate *in situ* SET-LRP. *J. Polym. Sci., Part A: Polym. Chem.* **49**, 4747–4755 (2011).

92. Abbas, S. S. *et al.* Facile silane functionalization of graphene oxide. *Nanoscale* **10**, 16231–16242 (2018).

93. Szabó, T., Berkesi, O. & Dékány, I. DRIFT study of deuterium-exchanged graphite oxide. *Carbon* **43**, 3186–3189 (2005).

94. Meng, D. *et al.* Grafting P3HT brushes on GO sheets: distinctive properties of the GO/P3HT composites due to different grafting approaches. *J. Mater. Chem.* **22**, 21583–21591 (2012).

95. Barrejón, M. *et al.* A photoresponsive graphene oxide–C_{60} conjugate. *Chem. Commun.* **50**, 9053–9055 (2014).

96. Avinash, M. B., Subrahmanyam, K. S., Sundarayya, Y. & Govindaraju, T. Covalent modification and exfoliation of graphene oxide using ferrocene. *Nanoscale* **2**, 1762–1766 (2010).

97. Su, W., Kumar, N., Krayev, A. & Chaigneau, M. In situ topographical chemical and electrical imaging of carboxyl graphene oxide at the nanoscale. *Nat. Commun.* **9**, 2891 (2018).

98. Lu, Y. *et al.* Novel blue light emitting graphene oxide nanosheets fabricated by surface functionalization. *J. Mater. Chem.* **22**, 2929–2934 (2012).

99. Melucci, M. *et al.* Facile covalent functionalization of graphene oxide using microwaves: bottom-up development of functional graphitic materials. *J. Mater. Chem.* **20**, 9052–9060 (2010).

100. Dave, S. H., Gong, C., Robertson, A. W., Warner, J. H. & Grossman, J. C. Chemistry and structure of graphene oxide via direct imaging. *ACS Nano* **10**, 7515–7522 (2016).

101. Thomas, H. R., Marsden, A. J., Walker, M., Wilson, N. R. & Rourke, J. P. Sulfur-functionalized graphene oxide by epoxide ring-opening. *Angew. Chem. Int. Ed.* **53**, 7613–7618 (2014).

102. Tararan, A., Zobelli, A., Benito, A. M., Maser, W. K. & Stéphan, O. Revisiting graphene oxide chemistry via spatially-resolved electron energy loss spectroscopy. *Chem. Mater.* **28**, 3741–3748 (2016).

103. Treossi, E. *et al.* High-contrast visualization of graphene oxide on dye-sensitized glass, quartz, and silicon by fluorescence quenching. *J. Am. Chem. Soc.* **131**, 15576–15577 (2009).

104. Layek, R. K., Samanta, S., Chatterjee, D. P. & Nandi, A. K. Physical and mechanical properties of poly(methyl methacrylate)-functionalized graphene/poly(vinylidine fluoride) nanocomposites: piezoelectric β polymorph formation. *Polymer* **51**, 5846–5856 (2010).

105. Liu, Z. *et al.* Direct observation of oxygen configuration on individual graphene oxide sheets. *Carbon* **127**, 141–148 (2018).

106. Li, H., Xue, S., Shang, Y., Li, J. & Zeng, X. Research and application progress based on the interfacial properties of graphene oxide. *Adv. Mater. Interfaces* **7**, 2000881 (2020).

107. Sharif, S., Ahmad, K. S., Rehman, F., Bhatti, Z. & Thebo, K. H. Two-dimensional graphene oxide based membranes for ionic and molecular separation: Current status and challenges. *J. Environ. Chem. Eng.* **9**, 105605 (2021).

108. Karki, N. *et al.* Functionalized graphene oxide as a vehicle for targeted drug delivery and bioimaging applications. *J. Mater. Chem. B* **8**, 8116–8148 (2020).

109. Lee, J., Kim, J., Kim, S. & Min, D.-H. Biosensors based on graphene oxide and its biomedical application. *Adv. Drug Delivery Rev.* **105**, 275–287 (2016).

110. Bhol, P. *et al.* Graphene-based membranes for water and wastewater treatment: a review. *ACS Appl. Nano Mater.* **4**, 3274–3293 (2021).

111. Yeh, C.-N., Raidongia, K., Shao, J., Yang, Q.-H. & Huang, J. On the origin of the stability of graphene oxide membranes in water. *Nat. Chem.* **7**, 166–170 (2014).

112. Zheng, S., Tu, Q., Urban, J. J., Li, S. & Mi, B. Swelling of graphene oxide membranes in aqueous solution: characterization of interlayer spacing and insight into water transport mechanisms. *ACS Nano* **11**, 6440–6450 (2017).

113. Chen, L. *et al.* Ion sieving in graphene oxide membranes via cationic control of interlayer spacing. *Nature* **550**, 380–383 (2017).

114. Mouhat, F., Coudert, F.-X. & Bocquet, M.-L. Structure and chemistry of graphene oxide in liquid water from first principles. *Nat. Commun.* **11**, 1566 (2020).

115. Wei, N., Peng, X. & Xu, Z. Understanding water permeation in graphene oxide membranes. *ACS Appl. Mater. Interfaces* **6**, 5877–5883 (2014).

116. Joshi, R. K. *et al.* Precise and ultrafast molecular sieving through graphene oxide membranes. *Science* **343**, 752–754 (2014).

117. Abraham, J. *et al.* Tunable sieving of ions using graphene oxide membranes. *Nat. Nanotechnol.* **12**, 546–550 (2017).

118. Hong, S. *et al.* Scalable graphene-based membranes for ionic sieving with ultrahigh charge selectivity. *Nano Lett.* **17**, 728–732 (2017).

119. Sun, P. *et al.* Selective ion transport through functionalized graphene membranes based on delicate ion–graphene interactions. *J. Phys. Chem. C* **118**, 19396–19401 (2014).

120. Park, H. B., Kamcev, J., Robeson, L. M., Elimelech, M. & Freeman, B. D. Maximizing the right stuff: the trade-off between membrane permeability and selectivity. *Science* **356**, eaab0530 (2017).

121. Ran, J. *et al.* Non-covalent cross-linking to boost the stability and permeability of graphene-oxide-based membranes. *J. Mater. Chem. A* **7**, 8085–8091 (2019).

122. Ji, J. *et al.* Osmotic power generation with positively and negatively charged 2D nanofluidic membrane pairs. *Adv. Funct. Mater.* **27**, 1603623 (2017).

123. Nie, L. *et al.* Realizing small-flake graphene oxide membranes for ultrafast size-dependent organic solvent nanofiltration. *Sci. Adv* **6**, eaaz9184 (2020).

124. Guan, K., Liu, G., Matsuyama, H.. & Jin, W. Graphene-based membranes for pervaporation processes. *Chin. J. Chem. Eng.* **28**, 1755–1766 (2020).

125. Chabot, V. *et al.* A review of graphene and graphene oxide sponge: material synthesis and applications to energy and the environment. *Energy Environ. Sci.* **7**, 1564–1596 (2014).

126. Luo, J. *et al.* Compression and aggregation-resistant particles of crumpled soft sheets. *ACS Nano* **5**, 8943–8949 (2011).

127. Kumar, M., Baniowda, H. M., Sreedhar, N., Curcio, E. & Arafat, H. A. Fouling resistant, high flux, charge tunable hybrid ultrafiltration membranes using polymer chains grafted graphene oxide for NOM removal. *Chem. Eng. J.* **408**, 127300 (2021).

128. Kong, F. *et al.* Rejection of pharmaceuticals by graphene oxide membranes: role of crosslinker and rejection mechanism. *J. Memb. Sci.* **612**, 118338 (2020).
129. Madadrang, C. J. *et al.* Adsorption behavior of EDTA-graphene oxide for Pb (II) removal. *ACS Appl. Mater. Interfaces* **4**, 1186–1193 (2012).
130. Mejias Carpio, I. E., Mangadlao, J. D., Nguyen, H. N., Advincula, R. C. & Rodrigues, D. F. Graphene oxide functionalized with ethylenediamine triacetic acid for heavy metal adsorption and anti-microbial applications. *Carbon* **77**, 289–301 (2014).
131. Zou, X., Zhang, L., Wang, Z. & Luo, Y. Mechanisms of the antimicrobial activities of graphene materials. *J. Am. Chem. Soc.* **138**, 2064–2077 (2016).
132. Lu, X. *et al.* Enhanced antibacterial activity through the controlled alignment of graphene oxide nanosheets. *Proc. Natl Acad. Sci. USA* **114**, E9793–E9801 (2017).
133. Ye, S. *et al.* Antiviral activity of graphene oxide: how sharp edged structure and charge matter. *ACS Appl. Mater. Interfaces* **7**, 21571–21579 (2015).
134. Yousefi, N., Lu, X., Elimelech, M. & Tufenkji, N. Environmental performance of graphene-based 3D macrostructures. *Nat. Nanotechnol.* **14**, 107–119 (2019).
135. Dekel, D. R. Review of cell performance in anion exchange membrane fuel cells. *J. Power Sources* **375**, 158–169 (2018).
136. Xiang, Y. *et al.* Advances in the applications of graphene-based nanocomposites in clean energy materials. *Crystals* **11**, 47 (2021).
137. Wang, C. *et al.* Graphene's role in emerging trends of capacitive energy storage. *Small*, 2006875 (2021).
138. Tian, Y. *et al.* Graphene oxide: an emerging electromaterial for energy storage and conversion. *J. Energy Chem.* **55**, 323–344 (2021).
139. Eftekhari, A., Shulga, Y. M., Baskakov, S. A. & Gutsev, G. L. Graphene oxide membranes for electrochemical energy storage and conversion. *Int. J. Hydrogen Energy* **43**, 2307–2326 (2018).
140. Yadav, R., Subhash, A., Chemmenchery, N. & Kandasubramanian, B. Graphene and graphene oxide for fuel cell technology. *Ind. Eng. Chem. Res.* **57**, 9333–9350 (2018).
141. Hatakeyama, K. *et al.* Proton conductivities of graphene oxide nanosheets: single, multilayer, and modified nanosheets. *Angew. Chem. Int. Ed.* **53**, 6997–7000 (2014).
142. Karim, M. R. *et al.* Effect of interlayer distance and oxygen content on proton conductivity of graphite oxide. *J. Phys. Chem. C* **120**, 21976–21982 (2016).

143. Tseng, C.-Y. *et al.* Sulfonated polyimide proton exchange membranes with graphene oxide show improved proton conductivity, methanol crossover impedance, and mechanical properties. *Adv. Energy Mater.* **1**, 1220–1224 (2011).
144. Jiang, Z., Zhao, X. & Manthiram, A. Sulfonated poly(ether ether ketone) membranes with sulfonated graphene oxide fillers for direct methanol fuel cells. *Int. J. Hydrogen Energy* **38**, 5875–5884 (2013).
145. Kumar, R., Mamlouk, M. & Scott, K. Sulfonated polyether ether ketone – sulfonated graphene oxide composite membranes for polymer electrolyte fuel cells. *RSC Adv.* **4**, 617–623 (2014).
146. Bao, C. *et al.* Graphene oxide beads for fast clean-up of hazardous chemicals. *J. Mater. Chem. A* **4**, 9437–9446 (2016).

Table 1 | **Main advantages and limitations of the derivatization reactions of GO**

Target functional group	Reaction or reagent	Advantages	Limitations	Refs
Epoxide	Nucleophilic ring opening	Mild conditions (no catalyst, can be performed in water and at room temperature)	Risk of partial reduction of GO when using basic nucleophiles[64]	61, 62, 63
Hydroxy	Silanization	Large choice of silanes	No use of amino- or thiol-terminated silanes	66
Hydroxy	Chlorosulfonic acid	Extensively used to prepare sulfated GO	No use of water for safety reasons	67
Hydroxy	Boronic acid	Mild conditions (no additional reagents, can be performed in water)	Limited to diols on GO	68
Hydroxy	Esterification	Large choice of carboxyl derivatives	–	72
Hydroxy	Isocyanate	No need of additional reagents	Side reaction with carboxyl groups on GO	73
Hydroxy	Williamson reaction	Mild conditions	No use of strong bases	72
Carboxyl	Esterification	High chemoselectivity compared with amidation	Low level of functionalization	75
C=C	Diazonium salt	Compatibility with many functional groups	Risk of oligomerization of the aryl radicals	77

GO, graphene oxide.

Table 2. **Applications and limitations of the most common techniques used to characterize functionalized GO**

Analytical technique	Information provided	Strengths	Limitations	Refs
XPS	Elemental surface composition; chemical environment of surface species	Quantification and information about functional groups grafted on GO	Peak deconvolution can be misinterpreted or overinterpreted	62, 83, 89

MAS NMR	Identification of the oxygenated groups of GO and molecules grafted on its surface	Epoxide, hydroxy and carbonyl groups have distinct peaks; possibility of quantitative ^{13}C NMR	Long acquisition time (several hours to days); requires specialists (to optimize parameters); rather large amount of sample needed (10–20 mg)	61, 63, 92
FTIR	Identification of molecules grafted on GO (measurement of vibrational modes)	Some bands can be assigned with high confidence, in particular in the range 2,000–3,000 cm^{-1}	Lack of sensitivity; risk of misinterpretation of the FTIR spectrum of GO; some assignments can be speculative	62, 63, 65, 74, 92, 94
Raman	Introduction of defects in GO (I_D/I_G ratio)	Can confirm covalent addition to the C=C bonds of GO	Not useful in the case of derivatization of the oxygenated groups; appearance of peaks specific to molecules grafted on GO is limited to Raman-active molecules	76, 83, 95-97
TGA	Thermal profile (weight loss as a function of temperature)	Possible to determine the number of molecules grafted on GO (in the case of heavy molecules); identification of molecules grafted on GO by TGA coupled to mass spectrometry or FTIR	Complex interpretation because of the thermal instability of GO; variability between measurements; control samples necessary	61, 63
AFM	Interlayer distance between GO sheets and lateral size dimensions	Can confirm the presence of bulky molecules on the surface of GO	Very sensitive to experimental and operating conditions (most atomic force microscopes require	103-105

			long and complex alignment procedures)	

AFM, atomic force microscopy; FTIR, Fourier-transform infrared; GO, graphene oxide; I_D and I_G, intensity of the D and G bands, respectively; MAS, magic-angle spinning; TGA, thermogravimetric analysis; XPS, X-ray photoelectron spectroscopy.

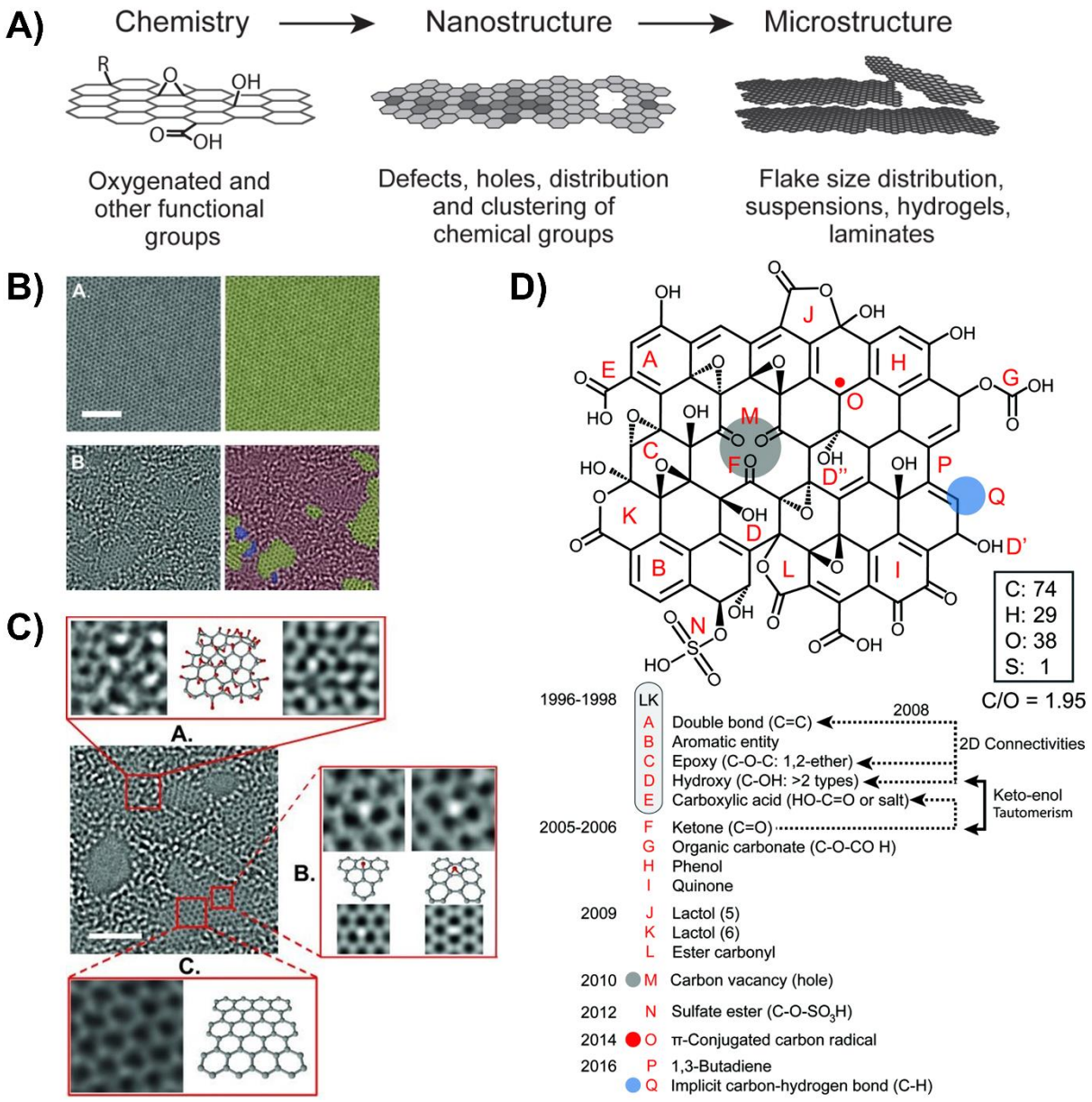

Fig. 1 | **Structure of graphene oxide. a** | The properties of graphene oxide (GO) materials depend on the details of their chemistry, nanoscale structure and microscale arrangements. **b** | Aberration-corrected high-resolution transmission electron microscopy (TEM) images of a suspended single sheet of graphene (top) and GO (bottom). On the right, graphitic areas are shown in yellow, holes in blue (usually <5 nm^2) and disordered, high-contrast oxidized areas in red (corresponding to approximately 16%, 2% and 82% of the area, respectively). Graphene is a 2D sp^2-hybridized carbon material, whereas GO has an inhomogeneous structure. **c** | Aberration-corrected TEM image of a suspended monolayer of GO. A GO sheet consists of nearly pure graphene domains separated by highly oxidized regions. Enlargement 1 shows a 1-nm^2 highly oxidized domain (left) and a

possible representative local atomic structure of this area (right; C and O atoms in grey and red, respectively). Enlargement 2 shows a 1-nm^2 graphitic region of GO (left) and the corresponding atomic structure (right). Enlargement 3 focuses on the white spot, which moved along the graphitic region, but stayed stationary for three frames (6 s) at a hydroxy position (top, left TEM image) and for seven frames (14 s) at a 1,2-epoxy position (top, right TEM image). The middle and bottom parts show the proposed atomic structures for these functionalities and corresponding simulated TEM images, respectively. **d** | Proposed structure of a GO sheet with a C/O ratio of ~2, based on different models (where LK is Lerf–Klinowski). The timeline shows the identification of the different functional groups and carbon vacancies. Panels **b** and **c** adapted with permission from ref.[25], Wiley-VCH. Panel **d** adapted with permission from ref.[4], Royal Society of Chemistry.

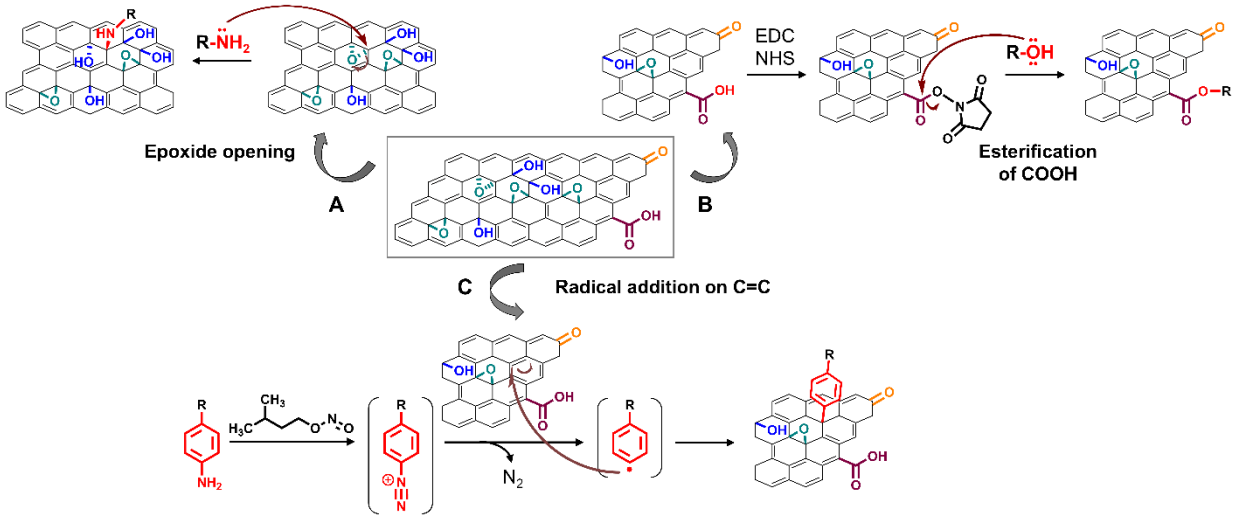

Fig. 2 | **Derivatization of the epoxide and carboxyl groups and C=C bonds of graphene oxide.** **a** | Epoxide ring opening by an amine derivative. **b** | Esterification of the carboxyl groups through reaction with an alcohol derivative in the presence of the coupling agents *N*-(3-dimethylaminopropyl)-*N′*-ethylcarbodiimide (EDC) and *N*-hydroxysuccinimide (NHS). The reaction proceeds via the formation of an activated ester. **c** | Addition of an aryl radical to a C=C bond. The aryl radical is generated from a diazonium salt, which is formed in situ from the reaction between the corresponding aniline and isoamyl nitrite in the presence of GO. Each reaction is shown on a fragment of a GO sheet and for only one functional group for clarity. Simplified mechanisms are illustrated.

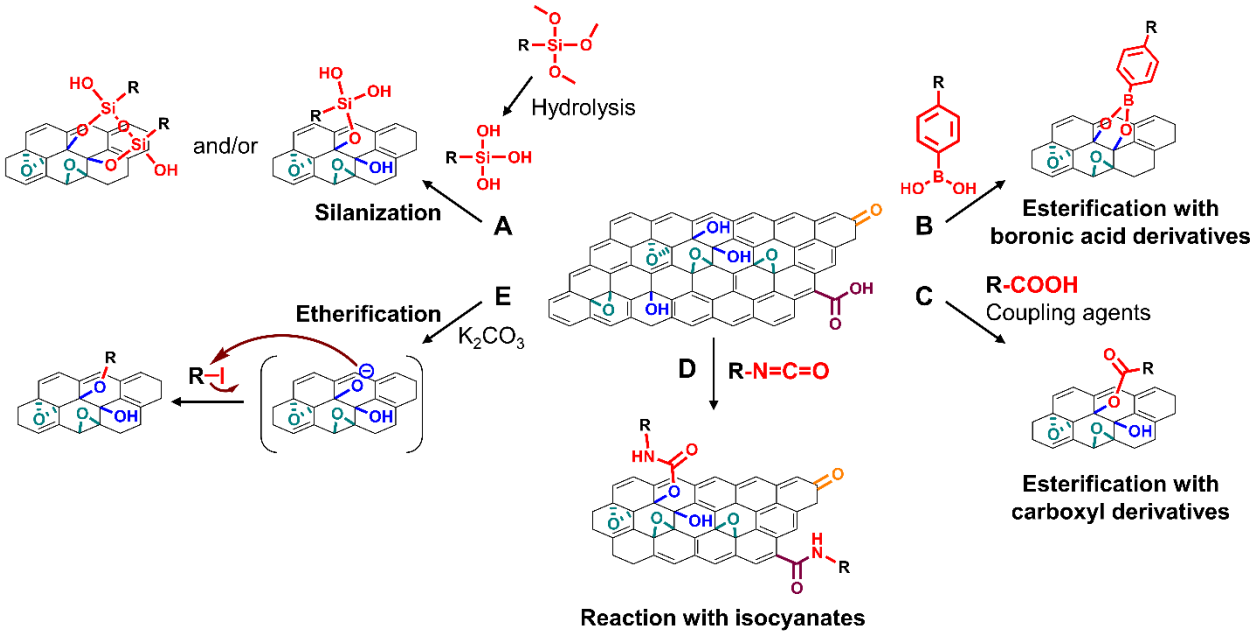

Fig. 3 | **Strategies for derivatizatizing of the hydroxy groups of graphene oxide. a** | Silanization of graphene oxide (GO). In this example, an alkoxysilane is first hydrolysed to form a silanol, which then reacts with the hydroxy groups on GO. Note that the possible nucleophilic attack of the silanol on the backside of the GO sheet is not shown here, because of the complex silanization mechanism. **b** | Reaction between a boronic acid derivative and a 1,2-diol moiety on GO to form a cyclic boronic ester. **c** | Reaction with a carboxyl derivative to form an ester bond. Coupling agents are required to activate the carboxyl group. **d** | Isocyanate derivatives can react with hydroxy groups on GO to form carbamates. However, isocyanates can also undergo a side reaction with carboxyl groups, making this reaction non-chemoselective. The mechanism is detailed in Fig. S2 in the Supplementary Information. **e** | Etherification (Williamson reaction) with a mild base (K_2CO_3) and an alkyl halide (RI). Each reaction is shown on a fragment of a GO sheet and for only one functional group for clarity. Simplified mechanisms are illustrated.

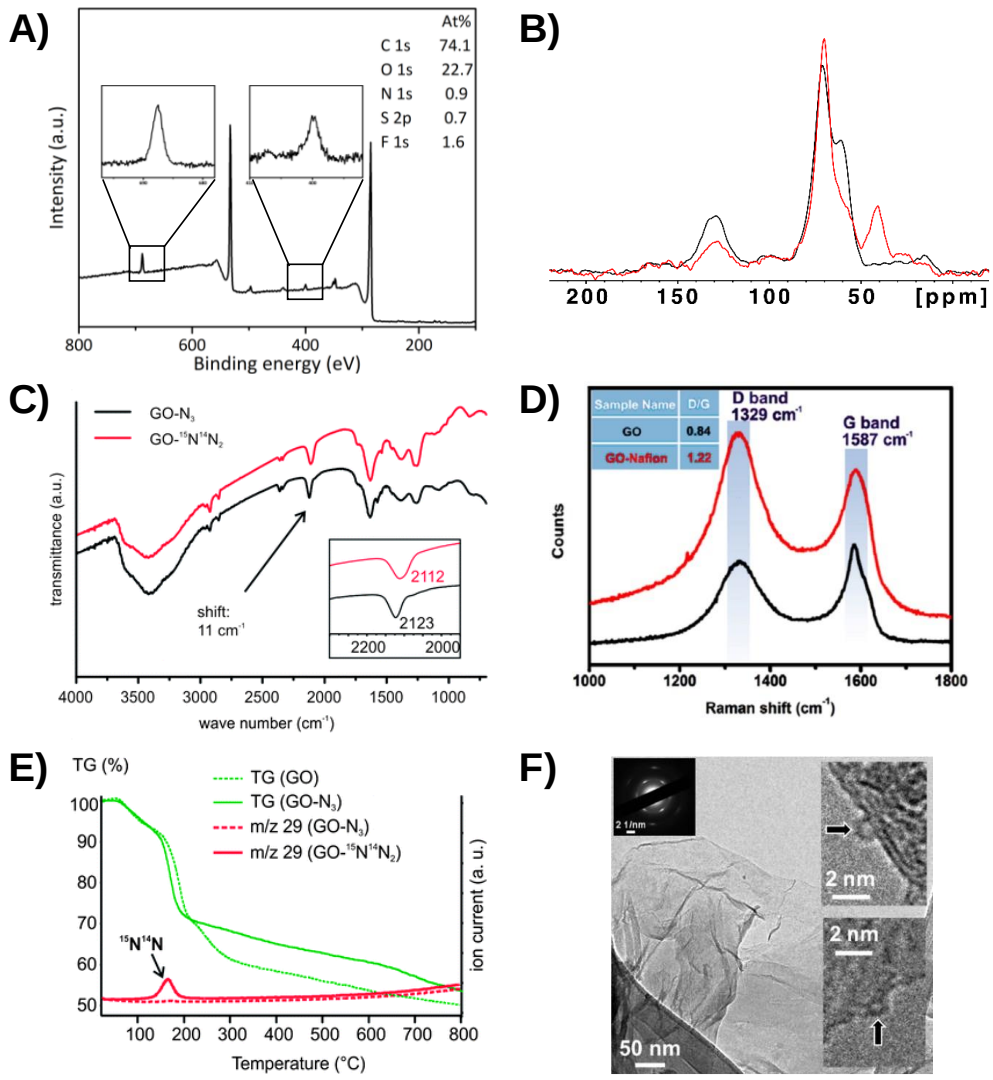

Fig. 4 | **Characterization of functionalized graphene oxide. a** | X-ray photoelectron spectroscopy survey spectrum of graphene oxide (GO) functionalized with Boc-aminoethanethiol (where Boc is *tert*-butyloxycarbonyl) and 3-(pentafluorothio)-phenylalanine. The left inset shows a magnification of the F 1*s* peak at ~688 eV and the right inset shows a magnification of the N 1*s* peak at ~400 eV. The table lists the calculated atomic percentages (At%). **b** | ^{13}C MAS NMR spectra of GO and GO functionalized with Boc mono-protected triethylene glycol diamine ('functionalized GO'). The relative intensity of the peak assigned to the epoxide groups at ~60 ppm decreases following functionalization. **c** | Fourier-transform infrared spectra of GO functionalized with sodium azide (GO–N_3) and with ^{15}N-labelled sodium azide (GO–$^{15}N^{14}N_2$). A 11 cm^{-1} shift is observed for the stretching vibration band of the azide at 2112 cm^{-1} (inset) when the reaction is performed using $Na^{15}N^{14}N_2$. **d** | Raman spectra of GO and GO functionalized with Nafion. In this case,

functionalization increases the ratio between the intensities of the D and G bands. **e** | Thermogravimetric analysis (TGA) curves of GO and GO–N_3 performed under an inert atmosphere and the mass-to-charge (*m*/*z*) 29 signal detected in the mass spectrometry analysis of the decomposition products of GO–N_3 and GO–$^{15}N^{14}N_2$. **f** | High-resolution transmission-electron microscopy images of GO functionalized with C_{60} and the corresponding selected area electron diffraction pattern (top left). C_{60} fullerenes are visible in the insets on the right (indicated by black arrows). Panel **a** adapted with permission from ref.[62], Wiley-VCH. Panel **b** adapted with permission from ref.[61], Royal Society of Chemistry. Panels **c** and **e** adapted with permission from ref.[63], CC BY 3.0 (https://creativecommons.org/licenses/by/3.0/). Panel **d** adapted with permission from ref.[83], Elsevier. Panel **f** adapted with permission from ref.[95], Royal Society of Chemistry.

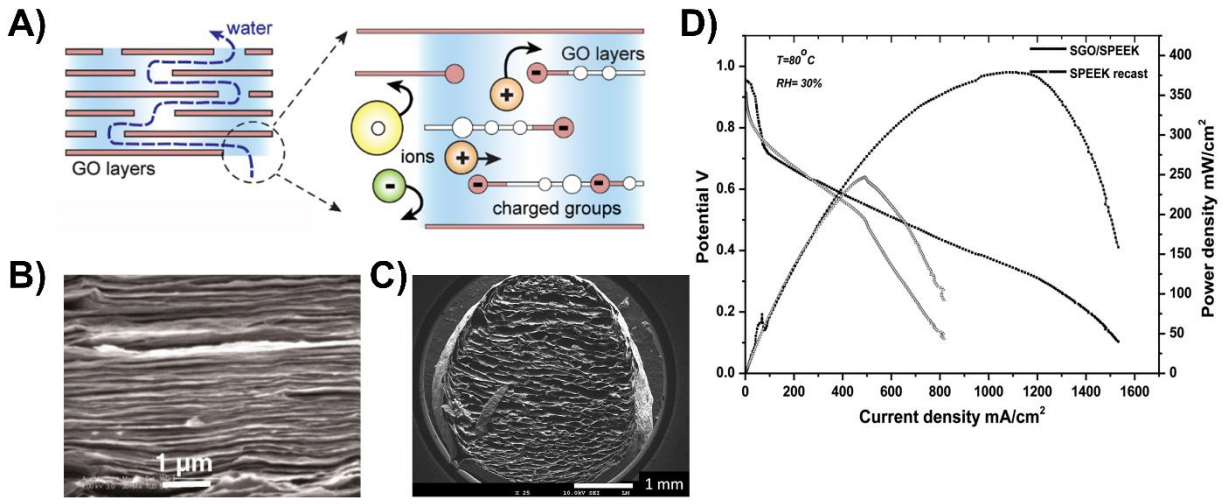

Fig. 5 | **Environmental and energy-related applications of functionalized GO. a** | For environmental applications of graphene oxide (GO) as separation membranes, the function is determined by the chemistry and hierarchical structure. Water transverses through a GO-based membrane, swerving around the flakes, while specific ions (positive, negative and neutral species shown in orange, green and blue, respectively) are rejected based on their charge (electrostatic forces) or their hydrated size compared to the interlayer spacing of GO (steric forces). **b** | Scanning electron microscopy (SEM) image of a cross section of a GO membrane consisting of layered GO flakes in a laminate structure with precise interlayer spacing. **c** | GO sorbents have controllable chemistry and a large surface area, as seen in the SEM image of a GO bead, to increase their adsorption capacity and specificity for contaminants. The bead comprises a GO foam core and an outer shell made from a GO membrane. **d** | Single-cell polarization curves of membrane electrode assemblies in which the membrane is either sulfonated poly(ether ether ketone) (SPEEK) or a composite comprising SPEEK and sulfonated GO (SGO) (at 80 °C and 30% relative humidity). The open-circuit voltage of the two membrane electrode assemblies is greater than 0.95 V, which is indicative of negligible gas crossover. The SPEEK–SGO composite membrane displays an enhanced fuel cell performance in comparison to SPEEK (with maximum power densities of 378 and 250 mW cm^{-2}, respectively). Panel **b** adapted with permission from ref.[12], AAAS. Panel **c** adapted with permission from ref.[146], Royal Society of Chemistry. Panel **d** adapted with permission from ref.[145], Royal Society of Chemistry.

Glossary terms

Epoxide

Three-membered C–O–C ring that possesses considerable strain, making them highly reactive towards nucleophiles.

Nucleophile

A species with an electron-rich atom that can donate an electron pair to form a new covalent bond.

Chemoselective

The selective reaction of a chemical reagent with a specific functional group without affecting others.

Multifunctionalization

Functionalization with multiple different functional groups; in the case of GO, this involves different oxygenated groups and/or the C=C bonds.

Carbanion

A molecule in which the carbon atom is trivalent (linked to three substituents) and bears a negative charge.

Electrophile

An electron-poor species that has a high affinity for electrons and can form covalent bonds by accepting electrons from a nucleophile.

Boronic acids

Trivalent boron-containing organic compounds with one alkyl or aryl substituent and two hydroxy groups.

1,2-Diol

Moiety with two hydroxy groups that occupy vicinal positions.

1,3-Diol

Moiety with two hydroxy groups separated by three carbon atoms.

Michael addition

Nucleophilic addition reaction of a carbanion (or nucleophile) to an α,β-unsaturated carbonyl compound that contains an electron-withdrawing group.

Wittig reaction

Reaction between an aldehyde or ketone with a triphenylphosphonium ylide, leading to the formation of an alkene.

Nafion

A sulfonated tetrafluoroethylene-based fluoropolymer-copolymer with excellent proton conductivity.